REASSESSING THE THERMAL HISTORY OF THE IAB PARENT ASTEROID USING W AND Pt ISOTOPES. A. C. Hunt[1], P. M. Reger[1], D. L. Cook[1], M. E. Ek[1] and M. Schönbächler[1]. [1]ETH Zürich, Institute for Geochemistry and Petrology, Clausiusstrasse 25, 8092 Zürich, Switzerland. E-mail: alison.hunt@erdw.ethz.ch.

Introduction: The ^{182}Hf-^{182}W chronometer ($_{t1/2}$ = 8.9 Ma) is a valuable tool that can effectively date metal-silicate separation in solar system bodies. The application of the ^{182}Hf-^{182}W chronometer, however, is hindered by the effects of neutron capture on W isotopes during exposure to galactic cosmic rays (GCR) [*e.g.* 1, 2]. Platinum is an ideal in-situ neutron dose proxy due to the similar neutron capture cross-sections of Pt and W [3]. Correlating GCR effects in W and Pt isotope compositions allows for an estimation of the pre-GCR exposure ε^{182}W, and consequently the timing of metal-silicate separation [4, 5, 6].

The IAB meteorites are non-magmatic iron meteorites. The thermal history and evolution of the IAB parent body remains unclear. One theory suggests that the IABs formed by crystal segregation in melt pools created by impacts [7, 8]. A competing theory argues that the decay of short-lived radionuclides (^{26}Al, ^{60}Fe) produced enough heat for incipient partial melting. This was followed by catastrophic impact and subsequent gravitational reassembly, which led to extensive mixing of silicates and metals [9, 10]. Several studies attempted to constrain the history of the IAB parent body using the ^{182}Hf-^{182}W chronometer [*e.g.* 1, 2, 11, 12]. These studies yielded a broad range of ages, which is partly related to difficulties to correct for GCR effects.

In this study, we report new W and Pt isotope data for the IAB irons to correct for GCR effects on W isotopes and to constrain the timing of metal-silicate separation on the IAB parent body. Our results provide new insights into the thermal evolution of the IAB body.

Methods: Fusion crust and weathered edges were first removed from the samples, prior to leaching in cold 2 M HCl. Samples were dissolved in a mixture of concentrated HNO_3 and HCl (2:1). Separate aliquots were then taken for Pt and W analysis. Platinum was purified as described by [13], and W was purified based on [14].

All isotopic analyses were made using a Thermo Scientific Neptune *Plus* MC-ICPMS fitted with a Cetac Aridus II desolvating system. Isotopic analyses were corrected for instrumental mass bias using the exponential law. Platinum isotope ratios were internally normalized using ^{198}Pt/^{195}Pt = 0.2145 [4]; mass bias for W was corrected using ^{186}W/^{184}W = 0.927672 [15]. Samples were measured relative to NIST SRM 3140 (Pt) or NIST SRM 3163 (W). Repeat analysis of two aliquots of the North Chile IIAB iron meteorite (an in-house reference material) gives an external reproducibility (2SD, n = 10) of 0.69 for ε^{192}Pt and 0.12 for ε^{196}Pt. These values are used as the uncertainty on individual samples. For ε^{182}W, the external reproducibility (2SD) is 0.08, based on replicate measurements of an NIST Fe-Ni steel (SRM 129c). Uncertainties on individual samples are based on the bracketing standard analyses (2SD) during the measurement session.

Results and Discussion. *Origin of Pt isotope variations:* Three samples (Caddo County, Canyon Diablo, Toluca) display Pt isotope compositions which overlap within uncertainty with the terrestrial value, whereas Cranbourne, Magura and Odessa show positive shifts for all Pt isotope ratios (Fig. 1). Irradiation of a meteoroid by GCR can alter Pt isotopes. Expected neutron capture effects on Pt isotopes were modelled by [3]. The IAB irons lie within uncertainty of the model line (Fig. 1). The Pt isotope deviations of all samples can be accounted for solely by GCR exposure. The good fit of the data to the GCR model also indicates that nucleosynthetic Pt isotope variations are absent, as previously recognised [4, 5, 6]. Additionally, the unexposed samples are identical to the terrestrial standard, and a regression line through the samples has an intercept at zero (Fig. 1), further arguing for the absence of nucleosynthetic anomalies.

Pre-exposure ε^{182}W: In diagrams of ε^{182}W vs. ε^{192}Pt and ε^{182}W vs. ε^{196}Pt, our data fall on well-defined linear trends (*e.g.* Fig. 2). The regression through our data and GCR model of [3] mostly overlap within uncertainty. The intercepts of the regression through the IAB samples at ε^{192}Pt and ε^{196}Pt = 0 yield pre-GCR exposure ε^{182}W [*e.g.* 4, 5, 6]. A weighted average of these two values yields a pre-exposure ε^{182}W of -2.93 ± 0.05. This indicates a time of metal-silicate separation in the IAB parent body of 5.6 ± 0.6 Ma after CAI formation. This is more precise, but in good agreement with other studies where no corrections for cosmogenic effects were applied, based on IAB samples which were only weakly exposed [1, 2, 12]. The age of 5.6 ± 0.6 Ma is significantly younger than those of the magmatic iron meteorites [4, 5, 6].

Of the five samples analysed, four (Canyon Diablo, Cranbourne, Magura and Odessa) belong to the IAB main group (MG), while Caddo County belongs to the Udei Station grouplet [8]. These groups are suggested to have formed through independent impacts into the parent body, forming distinct melt pools [7, 8]. These melt pools may have different metal-silicate separation ages, depending on the timing of the impact. Caddo

County, however, falls on the same trend as the other IABs. Therefore, the IAB-MG and Udei Station grouplet experienced contemporaneous metal-silicate differentiation. This argues for a single global thermal event. Our data cannot exclude that the two groups formed in separate melt pools induced by coeval impacts, but this relatively complicated scenario is not required by our data or thermal models (see below).

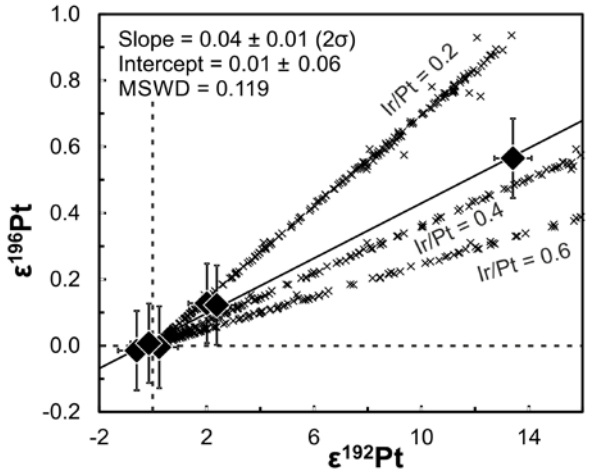

Figure 1: Plot of ε^{192}Pt vs. ε^{196}Pt for the IABs (diamonds). Also shown are the regression line through the data (Isoplot), and GCR model calculations [3] (black crosses; exposure time, 1000 Myr; variable Ir/Pt). The most appropriate Ir/Pt ratio for the IABs is 0.4 [8].

Evolution of the IAB parent body: Thermal models can help to constrain the relationship between timing of accretion and metal-silicate separation as well as parent body size (*e.g.* 16, 17). Thermal models incorporating internal heating by radioactive nuclides (mainly ^{26}Al and ^{60}Fe) indicate that a body with a radius > 50 km that accreted at ~1.7 - 2 Ma after CAI can reach the required temperatures for metal-silicate separation (~1250 K) at ~ 4 – 5 Ma after CAI [16, 17]. Therefore, the decay of short-lived radioactive nuclides can produce enough heat to explain the delayed metal-silicate separation of the IAB parent body. Nevertheless, the IAB parent body most likely experienced incomplete metal extraction and not true core formation, as indicated by trace-element concentrations [*e.g.* 8, 9]. Additionally, we cannot rule out a role for impacts into a pre-heated parent body.

Evidence also suggests an impact caused major disruption to the IAB parent body between 10 and 14 Ma after CAI [9, 10 and refs therein]. This event scrambled the IAB parent body, mixing molten metal and cool silicates. Such mixing requires a prolonged presence of molten metal. This is predicted by thermal models that consider a porous outer shell [17]. These shells can readily develop on late-formed planetesimals and act to insulate the body and hinder cooling, such that a body with a radius > 50 km may remain above the Fe, Ni – FeS cotectic in excess of 5 Myr [17].

Summary: In summary, Pt and W variations for the IAB irons are wholly due to exposure to GCR. A pre-GCR exposure ε^{182}W of -2.93 ± 0.05 can be derived and corresponds to a late metal-silicate separation age of 5.6 ± 0.6 Ma after CAI. Thermal models indicate that this event is early enough that short-lived radionuclides caused metal-silicate separation.

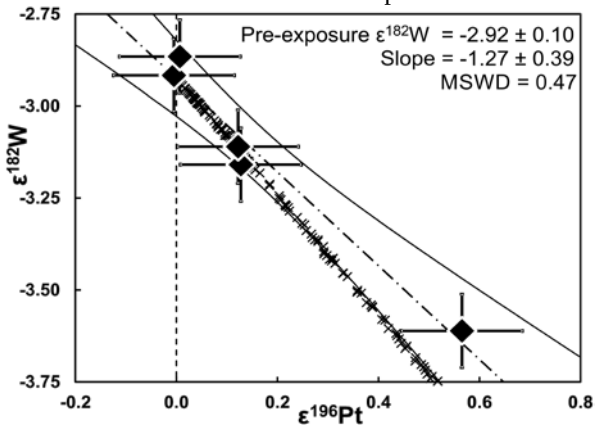

Figure 2: Correlation of ε^{196}Pt vs. ε^{182}W. The regression line and error envelope were plotted using Isoplot. Also shown are GCR model calculations [3] (black crosses; exposure time, 1000 Myr, Re/W=0.25, Os/W =3.125). The GCR model mainly lies within error of the regression line, but the model tends towards more negative ε^{182}W for larger ε^{196}Pt, as observed by [4].

References: [1] Kleine T. et al. (2005) *Geochim. Cosmochim. Acta*, 69, 5805-5818 [2] Markowski A. et al. (2006) *Earth. Planet. Sci. Letters*, 242, 1-15 [3] Leya I. and Masarik J. (2013) *Meteoritics & Planet. Sci.*, 48, 665-685 [4] Kruijer T.S. et al. (2013) *Earth. Planet. Sci. Letters*, 361, 162-172 [5] Wittig N. et al. (2013) *Earth. Planet. Sci. Letters*, 361, 152-161 [6] Kruijer T.S. et al. (2014) *Science*, 344, 1150-1154 [7] Choi B.-G. et al. (1995). *Geochim. Cosmochim. Acta*, 59, 593-612 [8] Wasson J.T. and Kallemeyn G.W. (2002) *Geochim. Cosmochim. Acta*, 66, 2445-2473 [9] Benedix G.K. et al. (2000) *Meteoritics & Planet. Sci., 35*, 1127-1141 [10] Theis K. et al. (2013) *Earth. Planet. Sci. Letters*, 361, 402-411 [11] Schulz T. et al. (2012) *Geochim. Cosmochim. Acta*, 85, 200-212 [12] Schulz T. et al. (2009) *Earth. Planet. Sci. Letters*, 280, 185-193 [13] Hunt A.C. et al. (2015) *LPSC 46*, Abstract #1835 [14] Cook D.L. et al. (2014) *Geochim. Cosmochim. Acta*, 69, 5805-5818 [15] Völkening J. et al. (1991) *Internat. J. Mass Spec. Ion Proc.* 107, 361-368 [16] Qin L. et al. (2008) *Earth. Planet. Sci. Letters*, 273, 94-104 [17] Lichtenberg T. et al. (2016) *Icarus*, in review